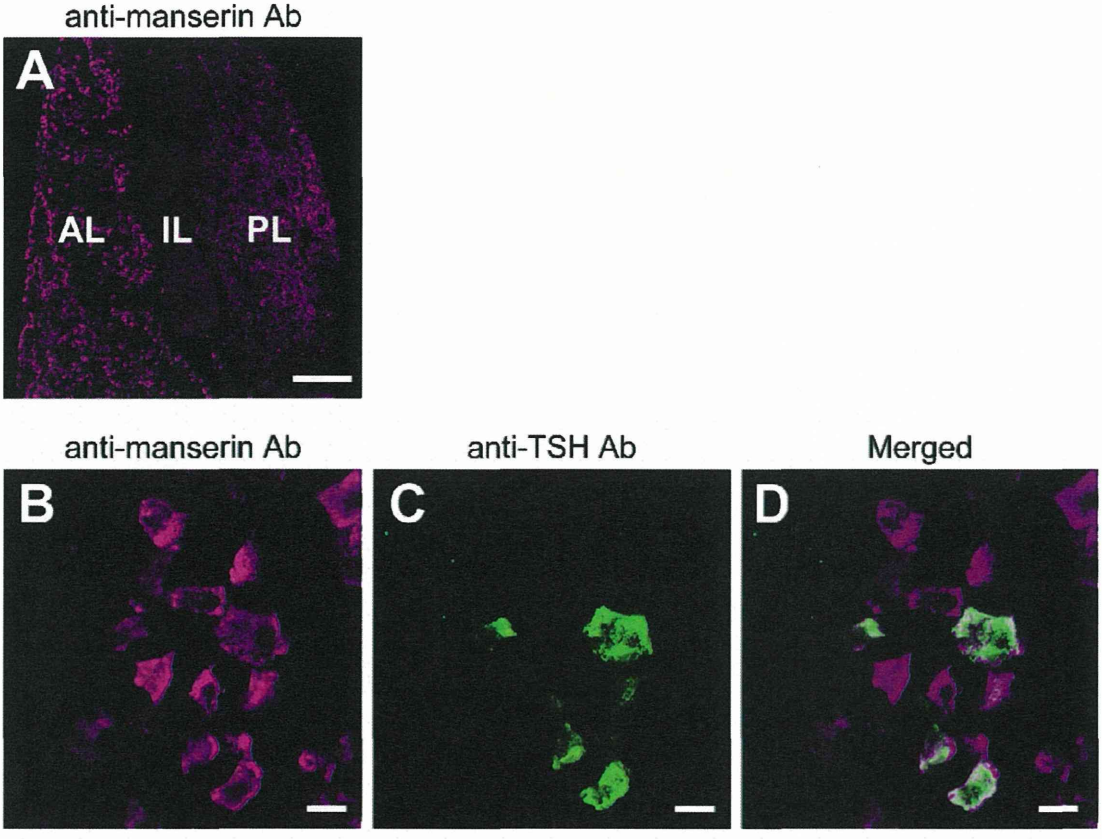

Fig. 1. Localization of manserin in TSH-expressing cells in the rat pituitary gland. Antigen–antibody complexes were detected by immunofluorescent staining (A–D). Manserin signals were detected in the anterior, intermediate, and posterior lobes of the pituitary gland (A). Double immunostaining with anti-manserin antibody (B) and anti-TSH antibody (C) was also shown. (D) is a merged image. AL, anterior lobe; IL, intermediate lobe; PL, posterior lobe. Scale bars = 200 μm (A) and 10 μm (B–D).

Tissue preparation

Anesthetized rats were transcardially perfused with 0.9% saline followed by perfusion with 4% paraformaldehyde (PFA) in phosphate buffered saline (PBS) (**Tano et al., 2010**). The thyroid and pituitary glands were dissected and immersed in 4.0% PFA in PBS overnight at 4 °C. For cryosectioning, the pituitary gland was cryoprotected in 30% sucrose, embedded in O.C.T. compound (Sakura Finetek, Tokyo, Japan), and sectioned at 9 μm thickness on a Leica CM1850 cryostat (Leica Microsystems, Wetzlar, Germany). For paraffin sectioning, the thyroid gland was immersed in a graded ethanol series and xylene and embedded in paraffin followed by sectioning at 7 μm using a rotary microtome.

Anti-manserin antibody

Affinity-purified rabbit anti-manserin antibody was prepared as described previously (**Kamada et al., 2010**). The specificity of the antibody was confirmed by immunoblotting (**Yajima et al., 2004**) and a preabsorption test.

Immunostaining

The thyroid and pituitary glands were immunostained as described previously (**Yajima et al., 2004, 2008**). In brief, sections were incubated in 3.0% H_2O_2 in PBS, washed with PBS, and blocked with 10% fetal bovine serum (FBS) in PBS containing 0.1% Triton X-100 for 1 h. The sections were then labeled with rabbit anti-manserin antibody overnight at 4 °C, incubated with biotin-conjugated anti-rabbit IgG (Chemicon, CA, USA), and washed with PBS. The sections were then stained by the ABC method and visualized with 3,3′-diaminobenzidine (DAB) using the Vectastain Elite ABC Kit (Vector Laboratories, Burlinghame, CA, USA). For counterstaining, sections of the thyroid gland were stained with Mayer's hematoxylin solution (Wako Pure Chemicals, Osaka, Japan).

Frozen sections of the pituitary gland were immunofluorescently stained as described previously (**Ohkawara et al., 2004; Tano et al., 2010**). For single immunostaining, the sections were incubated with anti-manserin antibody (**Kamada et al., 2010**) at 4 °C overnight. For double immunostaining, the sections were incubated with rabbit anti-manserin antibody (**Kamada et al., 2010**) and goat anti-thyroid-stimulating hormone (TSH) β chain antibody (Santa Cruz Biotechnology Inc., Santa Cruz, CA, USA) overnight at 4 °C, followed by incubation with fluorescently labeled secondary antibodies. Concentrations of secondary antibodies used in this study were as follows: Alexa 488-conjugated donkey anti-goat IgG (2 μg/ml; Invitrogen, Carlsbad, CA, USA) and Alexa 568-conjugated donkey anti-rabbit IgG (2 μg/ml; Invitrogen).

Paraffin sections of the thyroid gland were deparaffinized and rehydrated through a graded ethanol series. After rehydration, the sections were treated with citrate buffer (pH 6.0) for target retrieval, followed by blocking with 10% FBS in PBS containing 0.1% Triton X-100 for 1 h. The sections were then incubated with primary antibodies at 4 °C overnight, followed by incubation with fluorescently labeled secondary antibodies. Primary antibodies used for immunostaining of the paraffin sections were as follows: rabbit anti-manserin antibody (**Kamada et al., 2010**), rabbit anti-SgII antibody (QED Bioscience, San Diego, CA, USA), and goat anti-calcitonin antibody (Santa Cruz Biotechnology Inc.).

Please cite this article in press as: Ohkawara T, et al. Subtype-specific parafollicular localization of the neuropeptide manserin in the rat thyroid gland. Acta Histochemica (2012), http://dx.doi.org/10.1016/j.acthis.2012.05.003

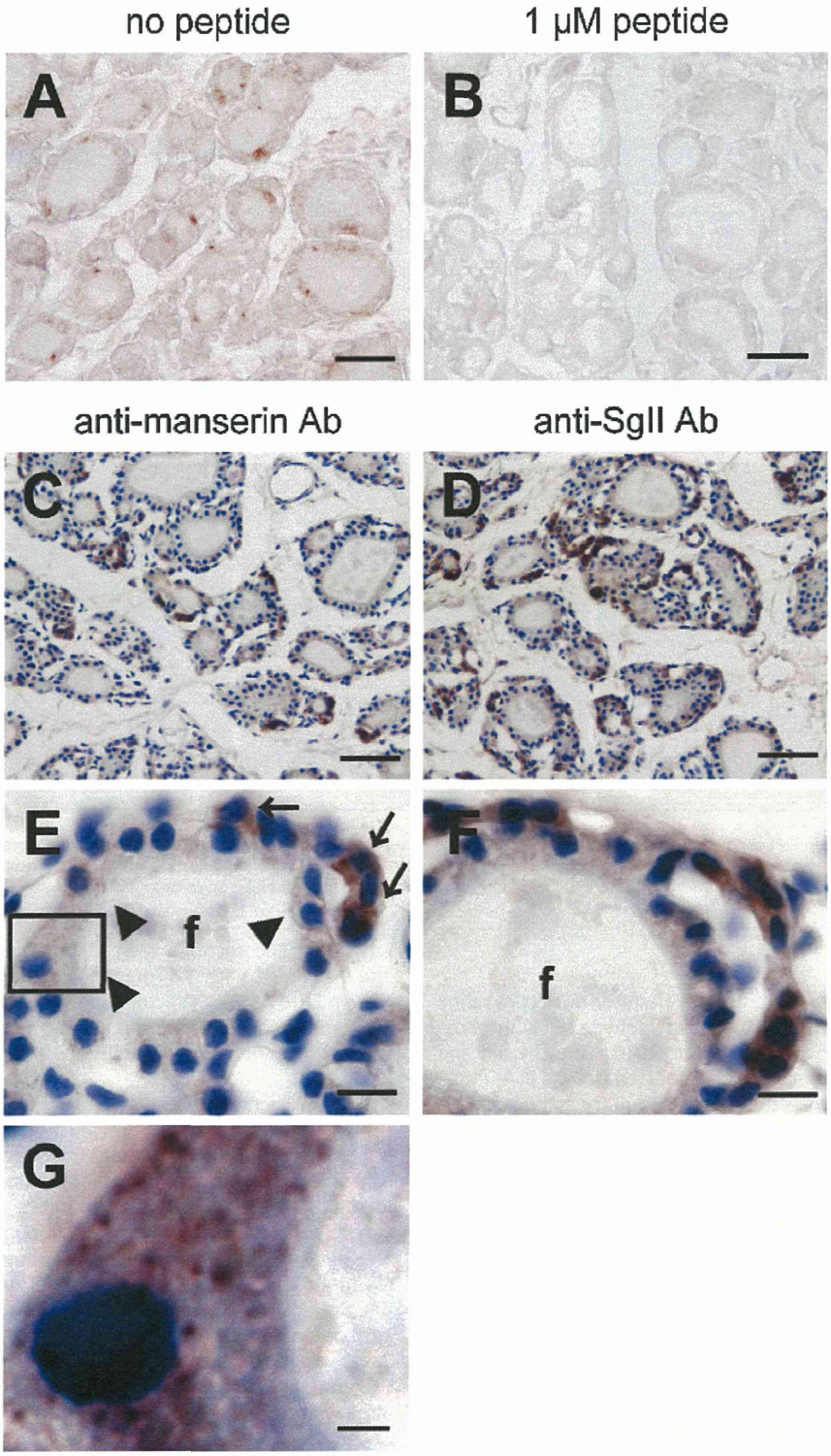

Fig. 2. Distribution of manserin in the thyroid gland. Antigen–antibody complexes were detected by DAB staining (*brown*, A–G). The specificity of anti-manserin antibody was confirmed by the preabsorption test. In the preabsorption test, manserin signals were detected when anti-manserin antibody was incubated with PBS (A), but no signal was detected when anti-manserin antibody was preabsorbed with a recombinant peptide (10^{-6} M) (B). In the thyroid gland, manserin signals (C, E and G) and SgII signals (D and F) were detected. *Arrows* in (E) indicate localization of manserin in the cells located in the interfollicular space. *Arrowheads* in (E) indicate localization of manserin in the follicular epithelial cells. (G) shows higher magnification view of the boxed area in (E). In (C)–(G), nuclei were counterstained with Mayer's hematoxylin solution. f, follicle. Scale bars = 50 μm (A–D), 10 μm (E and F) and 2 μm (G). (For interpretation of the references to color in this figure legend, the reader is referred to the web version of the article.)

Please cite this article in press as: Ohkawara T, et al. Subtype-specific parafollicular localization of the neuropeptide manserin in the rat thyroid gland. Acta Histochemica (2012), http://dx.doi.org/10.1016/j.acthis.2012.05.003

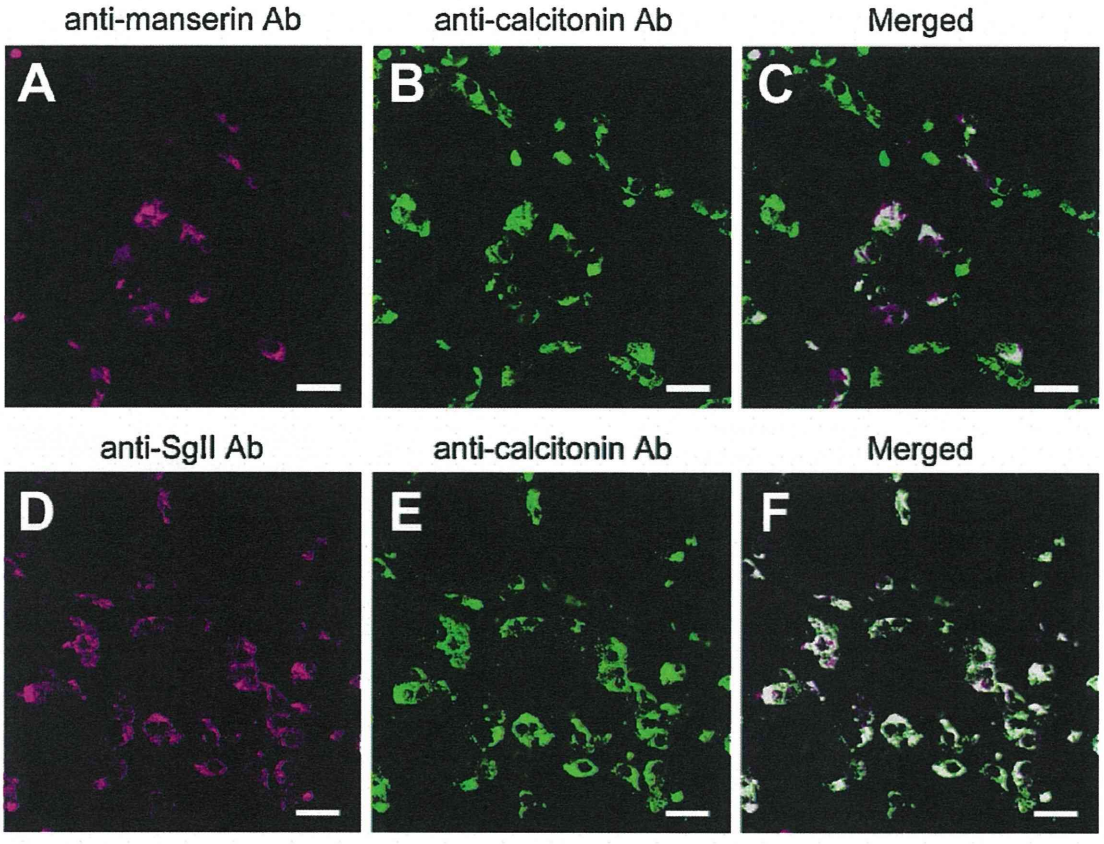

Fig. 3. Distribution of manserin or SgII in the parafollicular cells. Double immunostaining was performed with anti-calcitonin antibody (B and E) and anti-manserin (A) or anti-SgII antibody (D). Merged images are also shown (C and F). Scale bar = 20 μm (A–F).

Signals were visualized using an Olympus FV1000 laser scanning microscope (Olympus, Tokyo, Japan) for immunofluorescently stained sections and an Olympus BX50 microscope (Olympus, Japan) for sections stained by the ABC method. These images were processed using Adobe Photoshop CS5.1 (Adobe Systems Inc., CA, USA). Immunoreactive cells were counted using processed images.

Results

Because blood levels of thyroid hormones are controlled by TSH produced in the pituitary gland, we examined whether manserin was present in TSH-expressing cells in the rat pituitary gland. Manserin was detected in the anterior, intermediate, and posterior lobes of the pituitary gland (Fig. 1A). In our previous study, manserin was not localized in the intermediate and posterior lobes (Yajima et al., 2004). This apparent discrepancy may be explained because of (1) DAB staining, which is less sensitive than immunofluorescent staining and (2) anti-serum, but not affinity-purified anti-manserin antibody was used. Double staining with anti-manserin antibody and anti-TSH antibody revealed that manserin was present in TSH-expressing cells (Fig. 1B–D). The TSH-expressing cells were exclusively manserin positive, whereas only some manserin-positive cells were TSH positive (30.5% of 246 manserin-positive cells counted). Since manserin was colocalized with follicle stimulating hormone (FSH)-expressing cells (Yajima et al., 2004), cells that are manserin-positive and TSH-negative are thought to be FSH-expressing cells. These results indicate that manserin is present in TSH-expressing cells in the rat pituitary gland.

Because manserin is colocalized with the TSH-expressing cells in the pituitary gland as described above, the peptide is assumed to be localized in the thyroid gland. Intense, but scattered, manserin signals were observed in cells around follicles (Fig. 2A and C). At higher magnification, intense manserin-positive cells were exclusively localized in the space between follicles, i.e., the interfollicular space, suggestive of parafollicular cells (Fig. 2E, arrows). Under careful observation, manserin immunoreactivity was also observed in the follicular epithelial cells, although the immunostaining was less faint than parafollicular cells (Fig. 2E and G). These results indicate that manserin is present in follicular epithelial as well as in parafollicular cells. No signal was detected when the manserin antibody was preabsorbed with a recombinant peptide (10^{-6} M; Fig. 2B) and when the primary antibody was omitted (data not shown). SgII, a precursor of manserin that has been reported to be present in the thyroid gland (Schmid et al., 1992; Weiler et al., 1989), showed a staining profile quite similar to that of manserin (Fig. 2D and F).

To confirm the presence of manserin in parafollicular cells, we tested the colocalization of manserin with calcitonin, a parafollicular hormone that regulates blood Ca^{2+} levels. As reported (Foster, 1968), anti-calcitonin antibody stains almost all parafollicular cells (Fig. 3B and E). However, only 35.8% of 447 calcitonin-expressing cells counted were manserin positive (Fig. 3A and C), suggesting the existence of distinct forms of parafollicular cells. On the other hand, almost all (96.4%) of the calcitonin-expressing cells counted were SgII positive (Fig. 3D and F). These results suggest that manserin may localize only in a specific subtype of the parafollicular cells.

Discussion

This is the first study to demonstrate the presence of manserin in thyroid follicular epithelial cells and also in parafollicular cells.

Please cite this article in press as: Ohkawara T, et al. Subtype-specific parafollicular localization of the neuropeptide manserin in the rat thyroid gland. Acta Histochemica (2012), http://dx.doi.org/10.1016/j.acthis.2012.05.003

This result suggests that thyroid manserin may play some roles in the thyroid functions such as Ca^{2+} metabolism and hormone secretion.

We detected manserin signals as fine puncta in the cytoplasm of thyroid follicular epithelial cells. Because thyroid hormones are produced by the proteolytic cleavage of iodinated thyroglobulin in lysosomes and released by follicular epithelial cells into the blood, the punctate signals of manserin in the follicular epithelial cells indicate that manserin may reside in the lysosome where thyroid hormones were produced. Granin family proteins play a role in the formation of secretory vesicles (Iacangelo and Eiden, 1995; Kim et al., 2001), and there is evidence that the SgII-derived peptide SN is involved in stimulating the production and release of LH (Zhao et al., 2011). Thus, granin family proteins and their derived peptides play important roles in hormone secretion. Accordingly, we propose that manserin regulates the body metabolic rate by modulating thyroid hormone secretion, although further experiments are necessary to resolve this issue.

The presence of manserin in only approximately one-third of parafollicular cells indicates that manserin may be a marker for one subtype of the parafollicular cells. Sawicki (1995) reported that somatostatin was present in only a subset of these cells. The characterization of functionally different subtypes of the parafollicular cells awaits further studies of thyroid manserin.

The manserin precursor, SgII, was present in almost all parafollicular cells, whereas manserin was found in only one subset. Most parafollicular cells contain prohormone convertase (PC) 1 and PC2, which cleave precursor proteins including SgII at paired basic sites to yield bioactive peptides that include SN, EM66, and manserin (Kurabuchi and Tanaka, 2002). The same authors reported that PC2 was equally distributed in all of the parafollicular cells, but that the content of PC1 was different among the parafollicular cells. One possibility is that manserin is produced by the cleavage of SgII by PC1 and is accordingly found only in the parafollicular cells expressing relatively higher levels of PC1.

Manserin localizes in TSH-expressing cells and follicular epithelial cells in the pituitary and thyroid glands, respectively. TSH activates follicular epithelial cells and stimulates synthesis and secretion of thyroid hormones, T3 and T4 (Szkudlinski et al., 2002). The production and secretion of TSH are suppressed by blood levels of thyroid hormones. Thus, blood TSH levels are tightly controlled by a negative-feedback loop. The presence of manserin in TSH-expressing cells and follicular epithelial cells suggests that it plays a role in the maintenance of homeostasis using this negative-feedback mechanism. Further investigations of manserin are required to resolve this question. Since manserin was shown to be expressed depending on the stress (Kamada et al., 2010), homeostasis of calcium regulation depending on the stress is also thought to be maintained through manserin. Further studies using stress animals should be necessary to resolve this issue.

As a result of this study, we conclude that the novel peptide manserin is localized in TSH-expressing cells in the adult rat pituitary gland and in follicular epithelial cells in the thyroid gland. Although the manserin precursor protein SgII was found in almost all parafollicular cells, manserin was found in only approximately one-third of these cells. These results suggest that manserin performs subtype-specific functions in the parafollicular cells.

References

Cheng SY, Leonard JL, Davis PJ. Molecular aspects of thyroid hormone actions. Endocr Rev 2010;31:139–70.

Foster GV. Calcitonin (thyrocalcitonin). N Engl J Med 1968;279:349–60.

Iacangelo AL, Eiden LE. Chromogranin A: current status as a precursor for bioactive peptides and a granulogenic/sorting factor in the regulated secretory pathway. Regul Pept 1995;58:65–88.

Ida-Eto M, Oyabu A, Ohkawara T, Tashiro Y, Narita N, Narita M. Existence of manserin, a secretogranin II-derived neuropeptide, in the rat inner ear; relevance to modulation of auditory and vestibular system. J Histochem Cytochem 2012;60:69–75.

Kamada N, Tano K, Oyabu A, Imura Y, Narita N, Tashiro Y, et al. Immunohistochemical localization of manserin, a novel neuropeptide derived from secretogranin II, in rat adrenal gland, and its upregulation by physical stress. Int J Pept Res Ther 2010;16:55–61.

Kim T, Tao-Cheng JH, Eiden LE, Loh YP. Chromogranin A, an "on/off" switch controlling dense-core secretory granule biogenesis. Cell 2001;106:499–509.

Kurabuchi S, Tanaka S. Immunocytochemical localization of prohormone convertases PC1 and PC2 in the mouse thyroid gland and respiratory tract. J Histochem Cytochem 2002;50:903–9.

Ohkawara T, Oyabu A, Ida-Eto M, Tashiro Y, Tano K, Nasu F, et al. Secretogranin II and its derivative peptide, manserin, are differentially localized in Purkinje cells and unipolar brush cells in the rat cerebellum. Int J Pept Res Ther 2011;17:193–9.

Ohkawara T, Shintani T, Saegusa C, Yuasa-Kawada J, Takahashi M, Noda M. A novel basic helix–loop–helix (bHLH) transcriptional repressor, NeuroAB, expressed in bipolar and amacrine cells in the chick retina. Brain Res Mol Brain Res 2004;128:58–74.

Sawicki B. Evaluation of the role of mammalian thyroid parafollicular cells. Acta Histochem 1995;97:389–99.

Sawicki B, Zabel M. Immunocytochemical study of parafollicular cells of the thyroid and ultimobranchial remnants of the European bison. Acta Histochem 1997;99:223–30.

Schmid KW, Kirchmair R, Ladurner D, Fischer-Colbrie R, Böcker W. Immunohistochemical comparison of chromogranins A and B and secretogranin II with calcitonin and calcitonin gene-related peptide expression in normal, hyperplastic and neoplastic C-cells of the human thyroid. Histopathology 1992;21:225–32.

Spitzweg C, Heufelder AE, Morris JC. Thyroid iodine transport. Thyroid 2000;10:321–30.

Szkudlinski MW, Fremont V, Ronin C, Weintraub BD. Thyroid-stimulating hormone and thyroid-stimulating hormone receptor structure–function relationships. Physiol Rev 2002;82:473–502.

Tano K, Oyabu A, Tashiro Y, Kamada N, Narita N, Nasu F, et al. Manserin, a secretogranin II-derived peptide, distributes in the rat endocrine pancreas colocalized with islet-cell specific manner. Histochem Cell Biol 2010;134:53–7.

Weiler R, Cidon S, Gershon MD, Tamir H, Hogue-Angeletti R, Winkler H. Adrenal chromaffin granules and secretory granules from thyroid parafollicular cells have several common antigens. FEBS Lett 1989;257:457–9.

Yajima A, Ikeda M, Miyazaki K, Maeshima T, Narita N, Narita M. Manserin, a novel peptide from secretogranin II in the neuroendocrine system. Neuroreport 2004;15:1755–9.

Yajima A, Narita N, Narita M. Recently identified a novel neuropeptide manserin colocalize with the TUNEL-positive cells in the top villi of the rat duodenum. J Pept Sci 2008;14:773–6.

Yoo SH, Chu SY, Kim KD, Huh YH. Presence of secretogranin II and high-capacity, low-affinity Ca^{2+} storage role in nucleoplasmic Ca^{2+} store vesicles. Biochemistry 2007;46:14663–71.

Zhao E, McNeilly JR, McNeilly AS, Fischer-Colbrie R, Basak A, Seong JY, et al. Secretoneurin stimulates the production and release of luteinizing hormone in mouse LβT2 gonadotropin cells. Am J Physiol Endocrinol Metab 2011;301:E288–97.

Please cite this article in press as: Ohkawara T, et al. Subtype-specific parafollicular localization of the neuropeptide manserin in the rat thyroid gland. Acta Histochemica (2012), http://dx.doi.org/10.1016/j.acthis.2012.05.003

Journal of Neuroscience Research

Journal of Neuroscience Research 91:382–392 (2013)

Alterations in Local Thyroid Hormone Signaling in the Hippocampus of the SAMP8 Mouse at Younger Ages: Association With Delayed Myelination and Behavioral Abnormalities

Erika Sawano,[1] Takayuki Negishi,[1] Tomoyuki Aoki,[2] Masami Murakami,[2] and Tomoko Tashiro[1]*

[1]Department of Chemistry and Biological Science, Aoyama Gakuin University, Sagamihara, Kanagawa, Japan
[2]Department of Clinical Laboratory Medicine, Gunma University Graduate School of Medicine, Maebashi, Japan

The senescence-accelerated mouse (SAM) strains were established through selective inbreeding of the AKR/J strain based on phenotypic variations of aging and consist of senescence-prone (SAMP) and senescence-resistant (SAMR) strains. Among them, SAMP8 is considered as a model of neurodegeneration displaying age-associated learning and memory impairment and altered emotional status. Because adult hypothyroidism is one of the common causes of cognitive impairment and various psychiatric disorders, we examined the possible involvement of thyroid hormone (TH) signaling in the pathological aging of SAMP8 using the senescence-resistant SAMR1 as control. Although plasma TH levels were similar in both strains, a significant decrease in type 2 deiodinase (D2) gene expression was observed in the SAMP8 hippocampus from 1 to 8 months of age, which led to a 35–50% reductions at the protein level and 20% reduction of its enzyme activity at 1, 3, and 5 months. D2 is responsible for local conversion of thyroxine into transcriptionally active 3,5,3′-triiodothyronine (T3), so the results suggest a reduction in T3 level in the SAMP8 hippocampus. Attenuation of local TH signaling was confirmed by downregulation of TH-dependent genes and by immunohistochemical demonstration of delayed and reduced accumulation of myelin basic protein, the expression of which is highly dependent on TH. Furthermore, we found that hyperactivity and reduced anxiety were not age-associated but were characteristic of young SAMP8 before they start showing impairments in learning and memory. Early alterations in local TH signaling may thus underlie behavioral abnormalities as well as the pathological aging of SAMP8. © 2012 Wiley Periodicals, Inc.

Key words: thyroid hormone; SAMP8; type 2 deiodinase; hippocampus; hyperactivity; myelin basic protein

The senescence-accelerated mouse (SAM) strains were established through selective inbreeding of the AKR/J strain based on phenotypic variations of accelerated aging, such as amyloidosis, osteoporosis, and learning and memory deficits (Takeda et al., 1981). They consist of senescence-prone (SAMP) strains, which exhibit accelerated aging with a shorter life span, and senescence-resistant (SAMR) strains, which show normal aging. Among the SAMP strains, the SAMP8 strain displays mainly age-associated impairments in CNS function, including marked deficits in learning and memory (Miyamoto et al., 1986; Flood and Morley, 1992, 1993; Yagi et al., 1998), altered emotional status (Miyamoto et al., 1992; Markowaska et al., 1998), and abnormality of circadian rhythm (Miyamoto et al., 1986; Colas et al., 2005), with relatively mild physical impairments. Neuropathological and neurochemical studies have further shown that pathological changes observed in the aged brain such as increased oxidative stress, occurrence of Aβ-immunoreactive deposits (Del Valle et al., 2010), and neuroinflammation are detected earlier and at increased severity in the SAMP8 brain, especially in the

Contract grant sponsor: Ministry of Education, Culture, Sports, Science and Technology of the Japanese Government; Contract grant number: 20310037; Contract grant sponsor: High-Tech Research Center Project for Private Universities; Contract grant sponsor: Ministry of Health, Labor and Welfare of the Japanese Government (to T.T.).

*Correspondence to: Tomoko Tashiro, PhD, Department of Chemistry and Biological Science, Aoyama Gakuin University, 5-10-1 Fuchinobe, Chuo-ku, Sagamihara, Kanagawa, 252-5258 Japan.
E-mail: ttashiro@aoyamagakuin.jp

Received 2 February 2012; Revised 16 August 2012; Accepted 29 September 2012

Published online 6 December 2012 in Wiley Online Library (wileyonlinelibrary.com). DOI: 10.1002/jnr.23161

hippocampus, confirming the usefulness of this strain as a model for neurodegeneration (for review see Butterfield and Poon, 2005; Takeda, 2009; Tomobe and Nomura, 2009). The causes for such accelerated senescence, however, remain to be elucidated.

We focused on the thyroid hormone (TH) signaling as one potential contributing factor to accelerated aging in SAMP8, because TH plays essential roles not only in the developing brain (Oppenheimer and Schwartz, 1997; Koibuchi and Chin, 2000; Bernal, 2005; Williams, 2008) but also in the mature brain to maintain its proper functions. Adult hypothyroidism is one of the most common causes of transient dementia, and thyroid disorders have been linked to various psychiatric and neuropsychological disorders, including learning deficits, impaired attention, anxiety, and depression (for review see Davis and Tremont, 2007).

TH exerts its effects mainly through binding to the specific nuclear receptors of the steroid-retinoic acid-TH receptor superfamily, which function as ligand-regulated transcription factors (Oppenheimer and Schwartz, 1997; Koibuchi and Chin, 2000; Williams, 2008). The transcriptionally active form of TH that binds to these receptors is 3,5,3′-triiodothyronine (T3) produced by enzymatic deiodination of the initially synthesized form, thyroxine (T4). In addition to the well-known feedback system consisting of hypothalamus, pituitary, and thyroid gland (the HPT axis), which regulates the production of T4, it is now established that the concentration of T3 is locally regulated by three types of iodothyronine deiodinases; type 1 and 2 deiodinases (D1, D2), which convert T4 into active T3, and type 3 deiodinase (D3), which inactivates T3 (Gereben et al., 2008; Dentice and Salvatore, 2011). The T3-producing enzyme in the CNS is D2, which is expressed in astrocytes, whereas D3 is expressed in neurons.

In the present study, we examined the expression of D2 and D3 as well as representative TH-dependent genes to evaluate the local T3 availability in the hippocampus of SAMP8. The results indicate that, in spite of normal plasma TH level, the local TH signaling was significantly attenuated in the SAMP8 hippocampus from an early age (1 month) because of a significant reduction in D2 activity caused by a decrease at both mRNA and protein levels. At the same time, we found that, unlike the previously described behavioral abnormalities of SAMP8, hyperactivity and reduced anxiety were not age-associated but were characteristic of young SAMP8 (1–5 months), before they start showing symptoms of learning and memory impairment. Reduced local TH signaling starting during development may thus be a cause of abnormal behavior as well as accelerated aging of SAMP8.

MATERIALS AND METHODS

Animals

Male SAMP8 and SAMR1 mice were purchased from SLC (Shizuoka, Japan). They were housed individually under controlled temperature (24°C ± 1°C) on a 12-hr-light (06:00–18:00 hr):12-hr-dark (18:00–06:00 hr) cycle. Food and water were available ad libitum. To determine optimal conditions for the measurement of hippocampal iodothyronine deiodinase activity, 1-month-old male ICR mice (SLC) were used. All animal treatments were approved by the Animal Experimentation Committee of Aoyama Gakuin University and were carried out under veterinary supervision and in accordance with the Society for Neuroscience Guidelines for the use of animals in neuroscience research.

For one series of experiments, six mice each of SAMR1 and SAMP8 strains were used at 1, 3, 5, 8, and 10 months of age. After the behavioral tests described below, they were sacrificed under deep ether anesthesia. Blood samples were drawn from the heart and collected with EDTA as anticoagulant. After perfusion with phosphate-buffered saline (PBS), the brains were removed and separated sagitally into halves. In total five series of animals were used to obtain tissue samples for mRNA and protein extractions, measurement of enzyme activity, and immunohistochemical observation. For mRNA and protein extractions and enzyme activity measurements, hippocampi were removed, immediately frozen in liquid N_2, and kept at −80°C until use. For immunohistochemistry, brain halves were immediately fixed in 4% paraformaldehyde (PFA).

Passive Avoidance Test

Learning and memory abilities of SAMP8 and SAMR1 mice were examined at 1, 3, 5, 8, and 10 months by passive avoidance test using a two-compartment (light and dark) step-through cage (Muromachi Kikai Co., Tokyo, Japan). The tests were conducted between 6:00 and 10:00 PM. On the first day of examination (day 1), each mouse was placed in the light compartment, and the latency before entering the dark compartment (up to 60 sec) was measured. The mouse received an electrical shock (0.5 mA, 1 sec) immediately after entering the dark compartment. These trials were repeated up to five times until each mouse had learned to stay in the light compartment for at least 60 sec. On the next day (day 2), each mouse was placed in the light compartment, and the latency before entering the dark compartment (up to 300 sec) was measured.

Open-Field Test

Behavior and locomotor activity of SAMP8 and SAMR1 mice were examined at 1, 3, 5, 8 and 10 months by open-field test in a rectangular field (60 cm × 90 cm with walls of 45 cm height) with which all animals were unfamiliar. The tests were conducted between 6:00 and 10:00 PM. Each mouse was placed in the center of the field, and its behavior and locomotor activity were monitored for 5 min using a video camera and computerized analysis system (Smart System; Panlab, Barcelona, Spain).

Measurement of Plasma T4 and T3 Levels

Blood samples were centrifuged at 1,500*g* for 20 min at room temperature to obtain the plasma as the supernatant. T4 and T3 in the plasma from SAMP8 (n = 6) and SAMR1

TABLE I. Primers for Real-Time Quantitative PCR

	Forward	Reverse
ppia	GCAAGACCAGCAAGAAGATCACC	CTTCAGTGAGAGCAGAGATTACAG
dio2	CTACTACCTATGATCTGATTAAGTG	GGCTGGAACTAACACTTCAGTCC
dio3	CGACTACGCACAAGGGACCCG	CGATGTAGATGATAAGGAAGTCAAC
thra	CACCCCTATACACACAGAGAGC	GCCAAGCCAAGCCAAGCCAAG
thrb	CTATGACCCAGACAGCGAGACTC	CAGAGACATGCCCAGGTCAAAG
mct8	CATTCACAGGTCCCAGATCTGCCC	GCCCACACGTGCACACACGC
rc3	GACTTCCCTACTGTGTTTGTGAG	CTACGCCACGACGAAGCCAGC
hr	GCTGACCCCTCCCCTCATGG	GCAGTTGAGATACACAGAGGAAG
mbp	GGCACAGAGACACGGGCATCC	GCGACTTCTGGGGCAGGGAGC
enpp2	GTCAGAAAGGAATGGGGTCAACG	AGTGGGTAGGGACAGGAATAGAG

(n = 6) were measured by competitive enzyme-linked immunosorbent assay (ELISA) kit (Diagnostic Automation Inc.) according to the protocols recommended by the manufacturer.

Real-Time Quantitative Fluorescence-Based PCR

Total RNA was prepared individually from each hippocampus obtained from six mice of both strains at 1, 3, 5, 8, and 10 months using Trizol reagent (Invitrogen Life Technologies, Carlsbad, CA). The integrity of RNA samples was routinely monitored by microcapillary electrophoresis using a Bioanalyzer 2100 (Agilent Technologies, Palo Alto, CA). First-strand cDNA was synthesized from 1 μg total RNA from one animal using SuperScript III reverse transcription kit (Invitrogen Life Technologies). Expression levels of the following 10 genes in cDNA samples were quantified by fluorescence-based real-time PCR using Step One (Applied Biosystems, Foster City, CA) with SYBR Premix ExTaq (Takara, Shiga, Japan): cyclophilin-A (*ppia*), type 2 deiodinase (*dio2*), type 3 deiodinase (*dio3*), monocarboxylic acid transporter 8 (*mct8*), thyroid hormone receptor α (*thra*), thyroid hormone receptor β (*thrb*), neurogranine (*rc3*), hairless (*hr*), myelin basic protein (*mbp*), and ectonucleotide pyrophosphatase/phosphodiesterase 2 (*enpp2*). Cyclophilin-A (*ppia*) was used as an internal standard gene. PCR primers were designed in Oligo 6.0 primer analysis software (Molecular Biology Insights; Takahashi et al., 2008). Sequences of the PCR primers are listed in Table I.

Western Blotting

Each hippocampal sample obtained from SAMP8 or SAMR1 at 1, 3, 5, 8, and 10 months (n = 5–8 for either strain at each time point) was homogenized in 10 volumes of SDS sample buffer (0.06 M Tris-HCl, pH 6.8, 10% glycerol, 2% SDS, 0.04% bromophenol blue, 2% β-mercaptoethanol) containing protease inhibitors (Complete Mini EDTA-Free Protease Inhibitor Cocktail and PhosSTOP Phosphatase Inhibitor Cocktail; Roche Applied Science, Indianapolis, IN) using a glass-Teflon homogenizer, boiled at 100°C for 5 min, and centrifuged at 15,000*g* for 10 min at RT. Supernatants containing extracted proteins were collected and separated by SDS-PAGE on Tris-HCl gels followed by electrophoretic transfer onto polyvinyl difluoride (PVDF) membranes (Millipore, Bedford, MA). The blots were blocked for 1 hr at RT with 2% bovine serum albumin (BSA) or 2.5% skimmed milk in PBS containing 0.1% Tween 20 (PBS-T) and 0.02% sodium azide and incubated overnight at 4°C with one of the following primary antibodies in 2% BSA and 0.02% sodium azide-containing PBS: rabbit polyclonal anti-type 2 deiodinase (D2; 1:1,000; Abcam, Cambridge, United Kingdom), rabbit polyclonal anti-type 3 deiodinase (D3; 1:2,000; Novus Biologicals, Littleton, CO), chicken polyclonal anti-glial fibrillary acidic protein (GFAP; 1:20,000; Abcam), and monoclonal anti-β-actin (1:10,000; Sigma, St. Louis, MO). After being rinsed in PBS-T, the blots were incubated for 1 hr at RT with either of the following horseradish peroxidase (HRP)-conjugated secondary antibodies in 2% BSA with 0.02% sodium azide: anti-rabbit IgG (1:5,000), anti-chicken IgY (1:5,000), and anti-mouse IgG (1:10,000; all from Jackson Immunoresearch, West Grove, PA). The blots were rinsed several times in PBS-T and visualized by exposure to Hyperfilm ECL (GE Healthcare, Buckinghamshire, United Kingdom) using an Immobilon Western Chemiluminescent HRP Substrate (Millipore). For quantification, the films were scanned, and the density of each band was measured in Image J (National Institutes of Health).

Measurement of Iodothyronine Deiodinase Activity

Iodothyronine deiodinase activity was measured as previously described (Murakami et al., 1988), with minor modifications. To determine optimal conditions for the measurement of hippocampal D2 activity, iodothyronine deiodinase activity in the hippocampus of 1-month-old ICR mice was first characterized. Hippocampal samples were homogenized in homogenizing buffer (100 mM potassium phosphate, pH 7.0, containing 1 mM EDTA and 20 mM dithiothreitol) and centrifuged at 1,500*g* for 15 min at 4°C. The supernatants were incubated in a total volume of 50 μl containing various concentrations of [^{125}I]T4 (NEN Life Science Products Corp., Boston, MA), which was purified using LH-20 (Pharmacia Biotech, Uppsala, Sweden) column chromatography on the day of experiment, 1 mM EDTA, 20 mM dithiothreitol, in the presence or absence of 1 mM 6-propyl-2-thiouracil (PTU) or 1 mM iopanoic acid for 2 hr at 37°C. The reaction was terminated by adding 100 μl ice-cold 2% BSA and 800 μl ice-cold 10% trichloroacetic acid. After centrifugation at 1,500*g* for 10 min at 4°C, the supernatant was applied to a small column packed with AG 50W-X2 resin (bed volume 1 ml; Bio-Rad Laboratories, Hercules, CA) and then eluted with 2 ml of 10% glacial acetic acid. Separated ^{125}I was

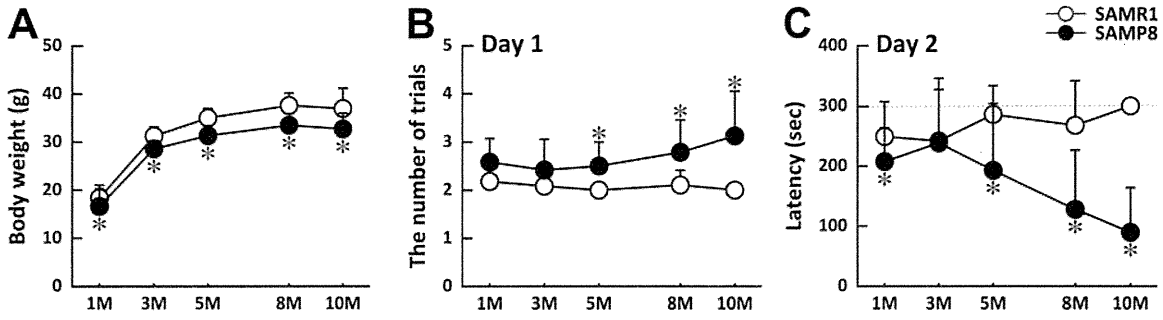

Fig. 1. Body weights and cognitive performances of SAMP8 and SAMR1 mice between 1 and 10 months. **A:** Body weights of SAMP8 (solid circles) and SAMR1 (open circles). **B,C:** Comparison of learning and memory abilities of SAMP8 (solid circles) and SAMR1 (open circles) by passive avoidance test at different ages. On day 1 (B), number of trials required before each mouse learned to stay in the light compartment for 60 sec was counted. On day 2 (C), latency time before each mouse entered the dark compartment (up to 300 sec) was measured. Results are expressed as means + SD. A: n = 21–59 (SAMR1), n = 14–55 (SAMP8). B,C: n = 8–15 (SAMR1), n = 8–12 (SAMP8). $^*P < 0.05$ between age-matched SAMP8 and SAMR1.

counted with a γ-counter. Nonenzymatic deiodination was corrected by subtracting I^- released in control tubes without homogenized samples. The protein concentration was determined by Bradford's method with BSA as a standard (Bradford, 1976). The deiodinating activity was calculated as fmol I^- released/mg protein/min, after multiplication by a factor of 2 to correct for random labeling at the equivalent 3′ and 5′ positions.

Each hippocampal sample from SAMP8 or SAMR1 was homogenized in 10 volumes of homogenizing buffer and centrifuged at 1,500*g* for 15 min at 4°C. Resultant supernatants were used for the measurement of D2 activity in the presence of 2 nM [^{125}I]T4, 1 mM EDTA, 20 mM dithiothreitol, and 1 mM PTU, as described above.

Immunohistochemistry

For immunohistochemical analysis, brain samples were fixed in 4% PFA for 48 hr at 4°C, dehydrated, embedded in paraffin, and cut into 8-μm-thick coronal sections. After deparaffinization and rehydration, the sections were incubated in 0.5% H_2O_2 for 20 min at RT to quench endogenous peroxidase activity, followed by 0.2% Triton X-100 for 15 min at RT. They were rinsed and incubated in 4% BSA for 30 min at RT to block nonspecific binding sites. Monoclonal anti-MBP antibody (1:1,000; Millipore) or monoclonal anti-S100 calcium binding protein B (S100β; 1:1,000; Sigma) was then applied to each section, and the sections were incubated overnight at 4°C. They were further rinsed and incubated with biotinylated secondary antibody (anti-mouse IgG; Chemicon/Millipore) at a dilution of 1:5,000 in BSA/PBS for 1 hr at RT. The sections were incubated in biotin-conjugated horseradish peroxidase with streptoavidin (ABC Elite Kit; Vector, Burlingame, CA) at a dilution of 1:1,000 for 30 min at RT and then visualized with nickel-intensified diaminobenzidine. The sections were counterstained with Carazzi's hematoxylin (Wako, Osaka, Japan), dehydrated and mounted in Entellan New (Merck, Darmstadt, Germany), and observed with a microscope (Axioplan 2; Carl Zeiss, Oberkochen, Germany).

Statistical Analysis

All numerical data were expressed as mean ± SD and analyzed by one-way ANOVA. When ANOVA revealed significant differences, it was followed by two-tailed Student's *t*-test. The level of significance was set at $P < 0.05$.

RESULTS

Confirmation of the Age-Associated Cognitive Impairment in SAMP8 Mice

SAMP8 mice were active and showed little physical impairment during the observation period of up to 10 months. They had slightly lower body weights (8.5–11.5%) compared with the age-matched SAMR1 (Fig. 1A). Progressive decline in learning and memory abilities of SAMP8 mice was confirmed by passive avoidance conditioning as shown in Figure 1B,C. Average number of trials necessary for learning on the first day of trial was significantly greater in SAMP8 mice compared with SAMR1 at 5, 8, and 10 months of age (125.0% at 5 months, 126.6% at 8 months, and 156.3% at 10 months of age-matched SAMR1), whereas memory retention represented by the latency before entering the dark compartment on the second day was progressively decreased in SAMP8 mice between 5 and 10 months (67.5% at 5 months, 48.6% at 8 months, and 29.9% at 10 months of age-matched SAMR1). Both of these parameters remained constant in SAMR1 between 1 and 10 months, indicating that SAMP8 mice became progressively impaired in learning and memory starting at about 5 months.

Behavioral Abnormalities of SAMP8 Mice Observed Prior to the Onset of Cognitive Decline

In addition to cognitive impairment, SAMP8 mice have been reported to exhibit behavioral abnormalities such as reduced anxiety that were also age dependent (Miyamoto et al., 1992; Markowska et al., 1998). With

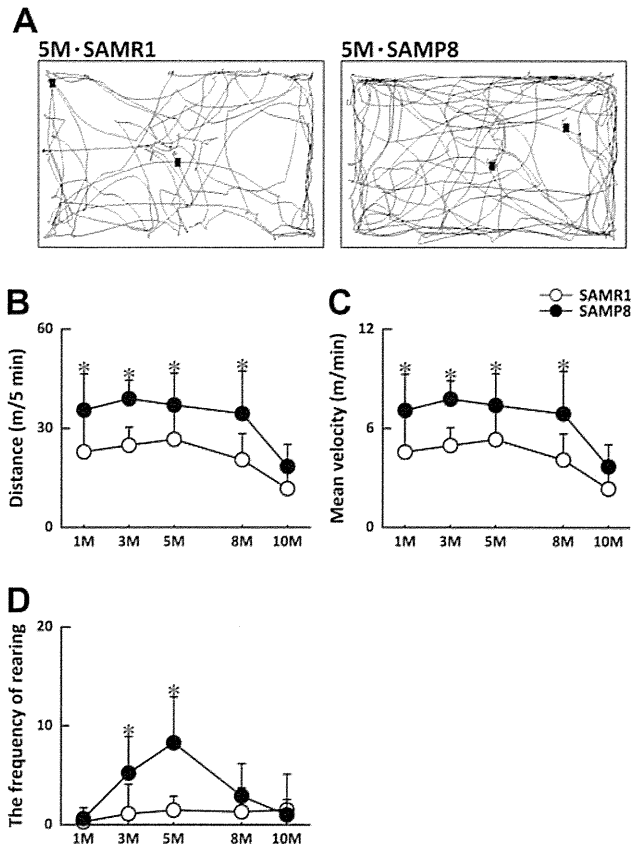

Fig. 2. Behavioral comparison of SAMP8 and SAMR1 mice by open-field test at different ages. **A:** Typical examples of trajectories of 5-month-old SAMR1 and SAMP8 in the first 5 min in an unfamiliar environment. Total distance (**B**), mean velocity during movement (**C**), and the frequency of rearing in the central part of the open field (**D**), recorded during the 5 min of test session. Results are expressed as means + SD [n = 13–30 for 1–8 months, n = 8 for 10 months (SAMR1), n = 10–28 for 1–8 months, n = 5 for 10 months (SAMP8)]. *$P < 0.05$ between age-matched SAMP8 and SAMR1.

the open-field test, however, we noted hyperactivity and reduced anxiety in young SAMP8 mice before they started showing cognitive decline, as shown in Figure 2. Typical examples of trajectories during the first 5 min of the test session in an unfamiliar environment are shown in Figure 2A for SAMR1 and SAMP8 at 5 months. Measurement of total distance traveled during the first 5 min demonstrated a significant increase in SAMP8 mice at 1, 3, 5, and 8 months compared with SAMR1 (Fig. 2B). Mean velocity during movement was also higher by ~30% in SAMP8 (Fig. 2C). In addition to such hyperactivity, rearing in the central part of the open field, interpreted as a sign of reduced anxiety, was frequently observed with SAMP8 mice at 3 and 5 months (Fig. 2D), whereas the frequency of rearing was minimal with SAMR1 at all ages.

TABLE II. Plasma Levels of Thyroxine (T4) and 3,5,3′-Triiodothyronine (T3) in SAMP8 and SAMR1 at Different Ages*

Age (months)	T4 (ng/ml)		T3 (ng/ml)	
	SAMR1	SAMP8	SAMR1	SAMP8
1	103.1 ± 14.4	109.4 ± 12.2	9.9 ± 0.7	9.4 ± 1.2
3	115.0 ± 15.0	103.5 ± 10.4	10.4 ± 0.7	10.9 ± 0.1
5	103.6 ± 20.3	115.8 ± 17.1	10.7 ± 0.2	10.4 ± 0.4
8	118.8 ± 19.1	98.4 ± 11.2	10.3 ± 1.7	10.8 ± 0.1
10	83.8 ± 15.9	110.3 ± 9.2	10.9 ± 0.2	10.6 ± 0.4

*Values are expressed as means ± SD [n = 6 (SAMR1), n = 6 (SAMP8)]. Plasma levels of T4 and T3 were comparable in the two strains at all ages examined.

Differences in the Expression of Genes Involved in Local TH Metabolism and Signaling in the Hippocampus of SAMP8 and SAMR1 Mice

To examine the possible involvement of TH signaling in the cognitive impairment and abnormal behaviors of SAMP8 mice, we first compared plasma TH levels of SAMP8 and SAMR1. As shown in Table II, plasma levels of T4 and T3 determined by ELISA were similar in both strains at all ages examined (1–10 months), indicating that the systemic TH status was not altered in SAMP8.

Because the level of transcriptionally active T3 in the CNS has been shown to be regulated locally, we next examined the expression of genes regulating local T3 availability as well as genes for its receptors in the hippocampus of SAMP8 and SAMR1 at different ages by real-time PCR. As shown in Figure 3A,B, significant differences between the two strains were observed in the mRNA expression of the two enzymes regulating the local T3 level. In the SAMP8 hippocampus, expression of the D2 gene (*dio2*), which converts T4 into active T3, was significantly downregulated at 1, 3, 5, and 8 months (Fig. 3A), whereas that of the D3 gene (*dio3*), responsible for inactivation of T3, showed a tendency to be upregulated (Fig. 3B) in comparison with SAMR1. The major neuronal TH transporter, monocarboxylate anion transporter 8 (*mct8*), was also significantly downregulated in SAMP8 at 3 months (Fig. 3C).

The mRNA expression of TH receptor α (*thra*) was similar in both strains at all time points (Fig. 3D), whereas TH receptor β (*thrb*) was significantly downregulated at 1 month and upregulated at 8 and 10 months in SAMP8 (Fig. 3E). Both of these TH receptors as well as *dio2* and *dio3* showed a peak of expression at 3 months, suggesting the importance of TH signaling at the maturation stage.

Reduction in D2 Protein and D2 Activity in the Hippocampus of SAMP8

Sustained reduction of *dio2* mRNA between 1 month and 5 months resulted in 35–50% reduction of the D2 protein in the hippocampus of SAMP8 compared with SAMR1 throughout the observation period, as shown in Figure 4A. In contrast, there was no differ-

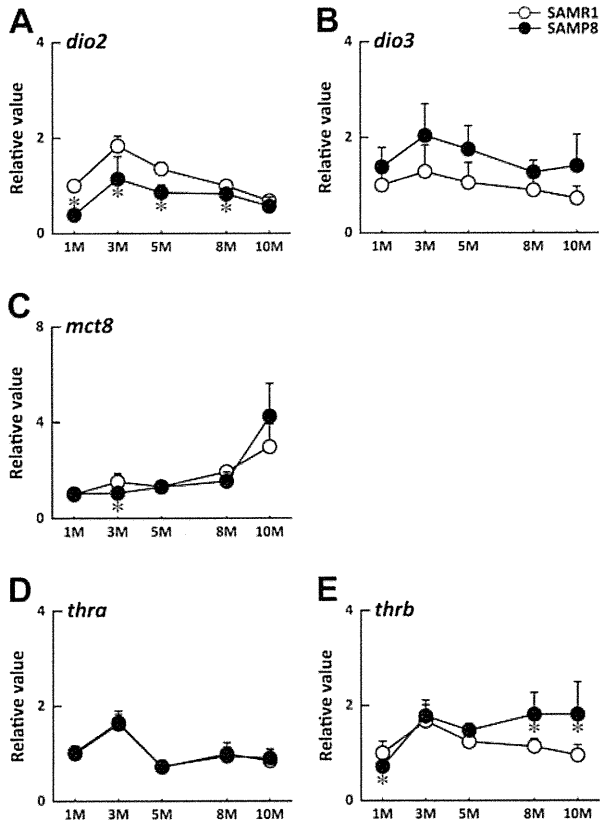

Fig. 3. Comparison of expression profiles of genes involved in TH metabolism and signaling in the hippocampus of SAMP8 and SAMR1. The mRNA expression of TH-metabolizing enzymes (**A:** *dio2*; **B:** *dio3*), a TH transporter (**C:** *mct8*), and TH receptors (**D:** *thra*; **E:** *thrb*) in the hippocampus of SAMP8 (solid circles) and SAMR1 (open circles) was quantified by real-time PCR at 1, 3, 5, 8, and 10 months using *ppia* as internal standard. Each mRNA level is expressed relative to that of SAMR1 at 1 month (means + SD of six mice/strain/age). $^{*}P < 0.05$ between age-matched SAMP8 and SAMR1.

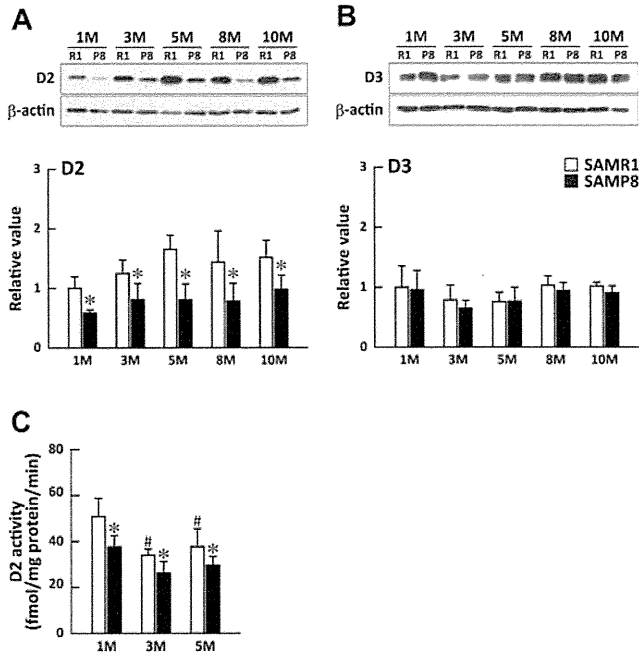

Fig. 4. D2 and D3 protein levels and D2 activity in the hippocampus of SAMP8 and SAMR1 at different ages. D2 (**A**) and D3 (**B**) protein levels quantified by Western blotting with anti-D2 and anti-D3 antibodies, respectively. Immunoreactive bands of D2 and D3 (examples shown in upper panels) in the hippocampus of SAMP8 (solid bars) and SAMR1 (open bars) at different ages were quantified using β-actin as standard and expressed relative to that of SAMR1 at 1 month. Results are expressed as means + SD [n = 6–8 (SAMR1), n = 5–6 (SAMP8)]. $^{*}P < 0.05$ between age-matched SAMP8 vs. SAMR1. **C:** D2 enzyme activity in the hippocampus of SAMP8 (solid bars) and SAMR1 (open bars) at 1, 3, and 5 months expressed as means ± SD [n = 6 (SAMR1), n = 5–6 (SAMP8)]. $^{*}P < 0.05$ between age-matched SAMP8 and SAMR1. $^{\#}P < 0.05$ compared with the value at 1 month of the same strain.

ence in D3 protein level between the two strains at all time points examined (Fig. 4B).

To compare further the D2 enzyme activity in the hippocampus of SAMR1 and SAMP8, iodothyronine deiodinase activity was first characterized with tissues from adult ICR mice. Hippocampal T4 deiodinating activity was not influenced by 1 mM PTU but was completely inhibited by 1 mM iopanoic acid. From the double reciprocal plot, kinetic constants for T4 were calculated to be K_m = 4.7 nM and V_{max} = 68 fmol I^- released/mg protein/min. These characteristics of iodothyronine deiodinase activity were compatible with D2 activity.

In the SAMR1 hippocampus, D2 activity was highest at 1 month and significantly decreased (21–29%) with maturation of the animal at 3 and 5 months. Compared with that in SAMR1, hippocampal D2 activity was confirmed to be reduced by 21–23% in SAMP8 at 1, 3, and 5 months (Fig. 4C).

Differences in the Expression of TH-Responsive Genes in the Hippocampus of SAMP8 and SAMR1 Mice

To determine whether TH signaling was affected in the SAMP8 hippocampus as suggested by the reduction in the availability of active T3, we next examined the mRNA expression of the following four known TH-dependent genes; neurogranin (*rc3*), myelin basic protein (*mbp*), hairless (*hr*), and ectonucleotide pyrophosphatase/phosphodiesterase 2 (*enpp2*). These genes are either equipped with the TH-responsive element (TRE) or have a great possibility of possession of TRE (Farsetti et al., 1991; Martínez de Arrieta et al., 1999; Potter et al., 2002; Freitas et al., 2010). Although the mRNA expression of *rc3* was similar in both strains (Fig. 5A), expression of *hr* at 1, 3, 5, and 8 months and *mbp* at all time points and of *enpp2* at 3 months were significantly downregulated in the hippocampus of SAMP8 compared with SAMR1 (Fig. 5B–D).

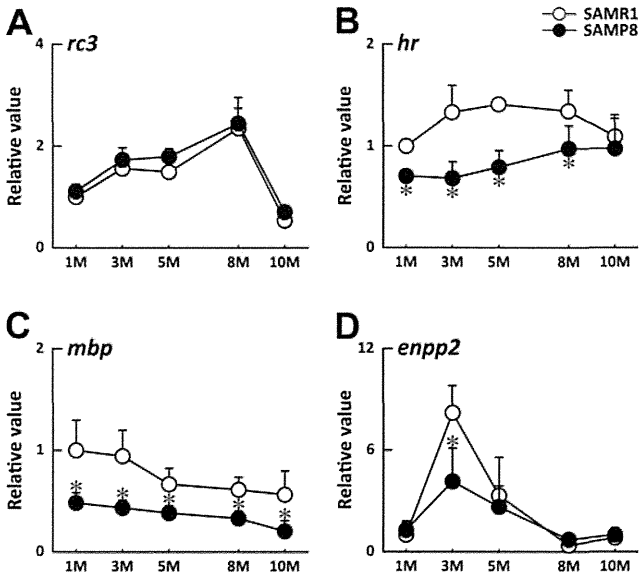

Fig. 5. Comparison of expression profiles of TH-responsive genes in the hippocampus of SAMP8 and SAMR1. The mRNA expression of *rc3* (**A**), *hr* (**B**), *mbp* (**C**), and *enpp2* (**D**) in the hippocampus of SAMP8 and SAMR1 was quantified by real-time PCR at 1, 3, 5, 8, and 10 months using *ppia* as internal standard. Each mRNA level is expressed relative to that of SAMR1 at 1 month (means + SD of six mice/strain/age). $*P < 0.05$ between age-matched SAMP8 and SAMR1.

Immunohistochemical Analysis of MBP Expression in the Hippocampus of SAMP8 and SAMR1 Mice

Because the mRNA expression of *mbp* in the SAMP8 hippocampus was significantly downregulated at all time points, we examined the expression of MBP protein by immunohistochemistry. As shown in Figure 6, prominent MBP immunoreactivity was observed in two regions of the hippocampus of both strains at all time points examined, one running along the stratum lacunosum-moleculare (open arrowheads in Fig. 6A) and the other running through the stratum radiatum of CA3 in a crescent shape (solid arrowheads in Fig. 6A). The former corresponds to the myelinated entorhinal projections (perforant path), and the latter corresponds mainly to the Schaffer collaterals, both of which are most intensively stained by other staining methods specific for myelin (Meier et al., 2004). The staining intensity appeared lower in SAMP8 compared with SAMR1 in these regions, especially at 1 month (Fig. 6A,B) and at 10 months (Fig. 6C,D). Quantification of total intensity of MBP immunoreactivity in two defined areas in the CA3 stratum radiatum (represented by squares a and b in Fig. 6E) at different time points showed a gradual increase in intensity up to 8 months in both strains (Fig. 6 F). Compared with that in SAMR1, MBP staining in SAMP8 was lower at 1, 3, and 8 months (Fig. 6F), suggesting a slower progression of myelination in the young SAMP8 mice, which never reached the level of SAMR1 at its maximum (8 months). Furthermore, a significant reduction in MBP intensity observed only in SAMP8 at 10 months indicates an earlier onset of age-related myelin loss in SAMP8.

Distribution and Morphology of Astrocytes in the Hippocampus of SAMP8 and SAMR1

Because D2 is localized to astrocytes, we further examined whether a reduction in D2 protein and activity simply reflected a decrease in astrocyte population or not. By immunohistochemical staining of astrocytic cell bodies with S100β (Fig. 7A–D), the number density of astrocytes in the hippocampus of the two strains was found to be similar and constant between 1 month and 10 months (Fig. 7E). In contrast, the amount of GFAP was significantly increased in SAMP8 at 5, 8, and 10 months compared with SAMR1 (Fig. 7F), in accordance with the morphological changes into reactive astrocytes (data not shown) as reported previously for aged SAMP8 mice (Nomura et al., 1996).

DISCUSSION

Altered Local T3 Signaling in the Hippocampus of the Young SAMP8 Mouse

In the present study, we show for the first time significant alterations in the expression profiles of TH-metabolizing enzymes in the hippocampus of young SAMP8 compared with SAMR1. In SAMP8, large reductions in the *dio2* mRNA level were observed between 1 month and 5 months, resulting in 35–50% reduction in the D2 protein level throughout the observation period (Figs. 3, 4) and significant reductions in D2 activity at 1 , 3, and 5 months (21–23%). On the other hand, D3 protein level was similar in both strains and was constant between 1 and 10 months.

Recent studies have established that TH signaling is precisely regulated locally by D2 and D3 activities (Dentice and Salvatore, 2011). The T3-degrading enzyme D3 is expressed mainly in fetal tissues, in which unoccupied TH receptors generally maintain cell proliferation and prevent premature differentiation (Williams, 2008). A rapid rise in T3 in mammals at birth is brought about by concomitant downregulation of *dio3* and upregulation of *dio2*. Postnatal expression of *dio3* is restricted to only a few tissues, including the brain, in which it is localized to neurons (Williams, 2008). Significant reduction in D2 protein and D2 activity with constant level of D3 protein observed in the present study thus suggests a decrease in the local availability of transcriptionally active T3 in the young SAMP8 hippocampus. Although it was not possible to assess the intracellular concentration of T3, weaker TH signaling in the SAMP8 hippocampus was confirmed by more than two-fold reductions in the expression of the three genes directly regulated by T3, especially at 3 and 5 months, when behavioral abnormalities of SAMP8 were most pronounced. Expression of one TH-responsive gene, *RC3/neurogranin*, was not altered in SAMP8,

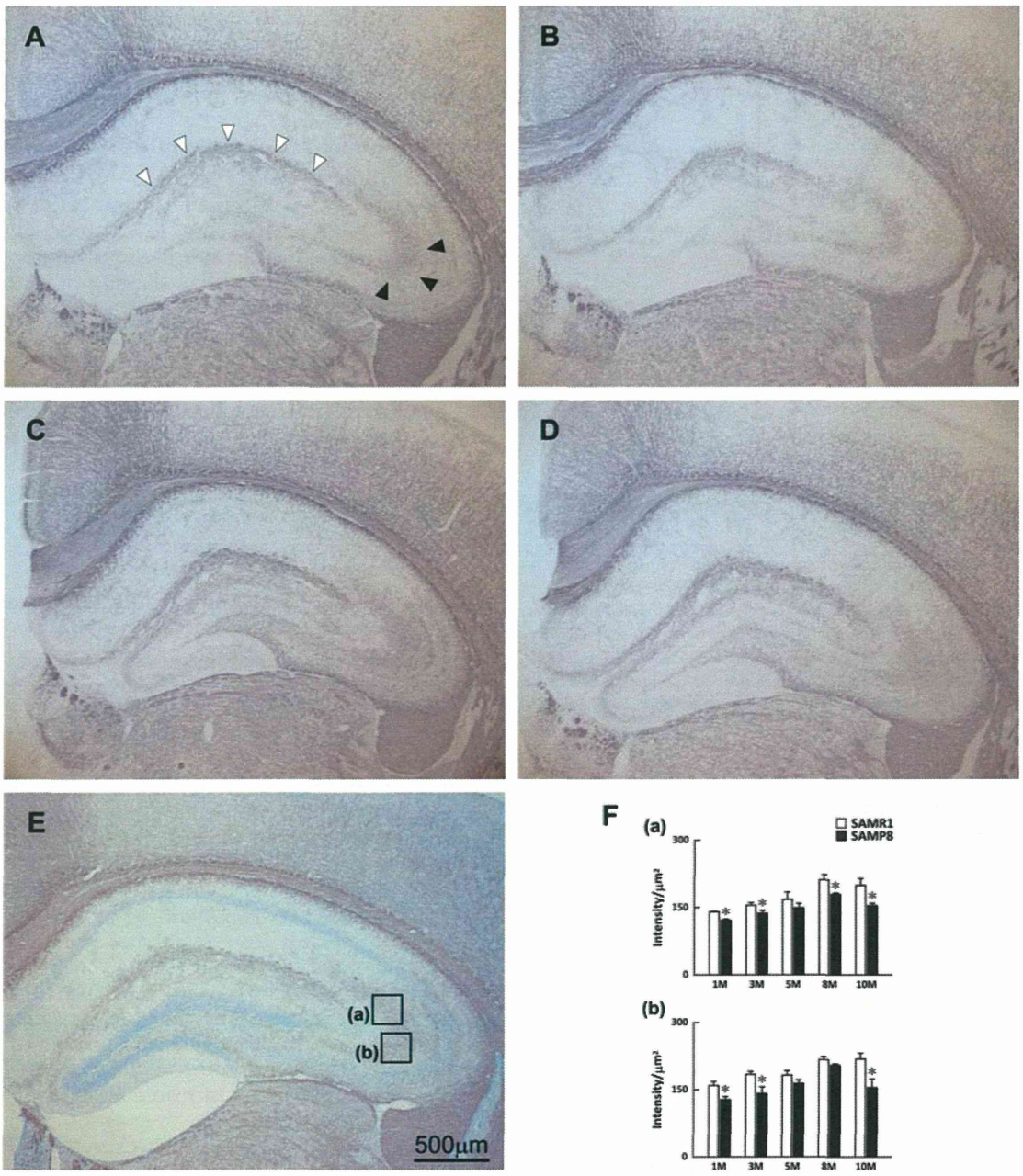

Fig. 6. Immunostaining with anti-MBP antibody in the hippocampus of SAMP8 and SAMR1 at different ages. Hippocampal sections (8 μm thick) from SAMP8 and SAMR1 aged 1, 3, 5, 8, and 10 months were stained with anti-MBP antibody. **A–D** show sections from SAMR1 (A) and SAMP8 (B) at 1 month and SAMR1 (C) and SAMP8 (D) at 10 months. Open arrowheads, stratum lacunosum-moleculare; solid arrowheads, stratum radiatum of CA3. In **E**, a section from SAMR1 at 5 months counterstained with hematoxylin is shown. **F:** Total intensity of MBP immunoreactivity in two defined areas in CA3 (represented by the two squares in E) was quantified individually at different time points. Results are expressed as means + SD. Three sections per mouse and three mice/strain/age were analyzed. $^*P < 0.05$ between age-matched SAMP8 and SAMR1.

probably because this gene for the postsynaptic protein is abundantly expressed only between 1 and 2 weeks postnatally.

Further studies are needed to determine the causes of the reduction of D2 protein and D2 activity in SAMP8 mice. D2 is an endoplasmic reticulum

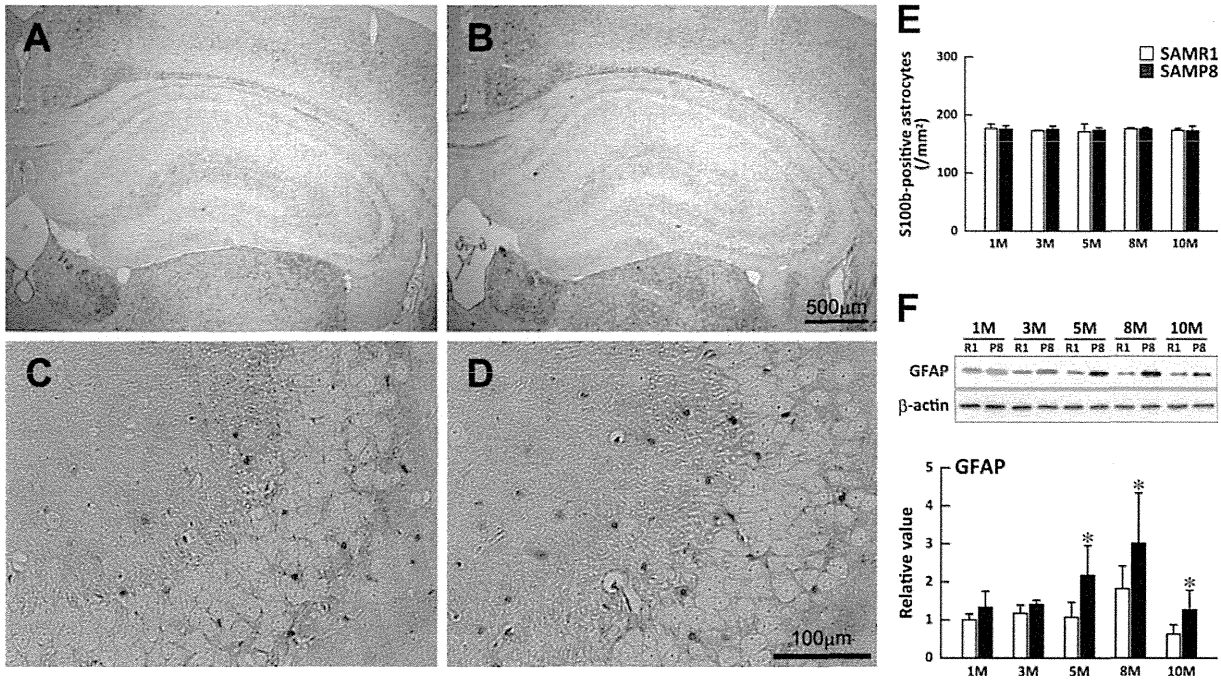

Fig. 7. Astrocyte density and GFAP content of the SAMP8 and SAMR1 hippocampus at different ages. Astrocyte cell bodies were visualized by immunostaining with anti-S100B antibody in the whole hippocampus (**A,B**) and CA3 region (**C,D**) of SAMR1 (A,C) and SAMP8 (B,D) mice at 3 months. **E:** Number densities of astrocytes in the whole hippocampus of SAMR1 (open bars) and SAMP8 (solid bars) were obtained by counting S100B-positive cell bodies at different ages and expressed as mean + SD [n = 3–8 (SAMR1, SAMP8)]. **F:** GFAP content of the SAMR1 (open bars) and SAMP8 (solid bars) hippocampus quantified by Western blotting with anti-GFAP antibody. Immunoreactive bands of GFAP (examples shown in the upper panel) at different ages were quantified using β-actin as standard and expressed relative to that of SAMR1 at 1 month. Results are expressed as means + SD [n = 5–8 (SAMR1), n = 5–6 (SAMP8)]. $^*P < 0.05$ between age-matched SAMP8 and SAMR1.

(ER)-resident protein in astrocytes and tanycytes regulated posttranslationally by ubiquitination-dependent inactivation and degradation, which are enhanced by T4 (for review see Arrojo e Drigo and Bianco, 2011). Because the densities of S100B-positive astrocytes were similar and constant with age in both strains and GFAP immunoreactivity in the SAMP8 hippocampus was comparable to that in SAMR1 up to 3 months (Fig. 7), we can rule out the possibility that the reduction in D2 protein simply reflects a decrease in astrocyte population. At the transcriptional level, *dio2* has been shown to be downregulated by oxidative stress and inflammation, whereas *dio3* is upregulated (Lamirand et al., 2008; Simonides et al., 2008; Calzà et al., 2010). Such reciprocal changes in the expression of *dio2* and *dio3* in response to pathological conditions lead to reduced local T3 concentration, which in turn should decrease metabolic activity and prevent further production of oxidative stress. Reduced expression of *dio2* in SAMP8 at older ages may arise from elevated oxidative stress (Butterfield et al., 1997; Tomobe et al., 2012) or chronic expression of proinflammatory cytokines such as interleukin (IL)-1β, IL-6, and tumor necrosis factor-α (Tha et al., 2000) reported for SAMP8 at 10 months. On the other hand, an explanation for the severe downregulation of *dio2* at earlier time points (1 and 3 months) awaits further studies on the perinatal development of the TH system of SAMP8.

Delayed Myelination Followed by Earlier Onset of Myelin Degeneration in the SAMP8 Hippocampus

In addition to signs of oxidative stress (Butterfield et al., 1997) and increased amyloid β burden (Del Valle et al., 2010), loss of myelin and myelinating oligodendrocytes have been previously reported for the brains of old SAMP8 (10 months of age; Tanaka et al., 2005). The present study reveals that there is already an impairment of myelination during development.

It is well established that TH plays a critical role in developmental myelination, both through regulation of oligodendrocyte differentiation and through expression of myelin component genes such as *mbp* (Oppenheimer and Schwartz, 1997; Koibuchi and Chin, 2000). Importance of TH in remyelination in the adult CNS has also been highlighted in recent studies on inflammatory-demyelinating diseases in which immune activation and brain injury downregulate *dio2* and lead to a decrease in local T3 availability (Calzà et al., 2005, 2010). A decrease in MBP immunoreactivity observed in SAMP8

at later time points (10 months) may result from downregulation of *dio2* by oxidative stress and/or by proinflammatory cytokines.

Possible Relationship Between TH Deficiency and Abnormal Behavior of Young SAMP8 Mice

In addition to the age-associated cognitive impairment, behavioral abnormalities of SAMP8 mice have been described in an earlier study by Miyamoto et al. (1992), in which the authors detected lower anxiety in an elevated plus maze test, food neophobia, and punished drinking test. These behavioral characteristics were noted at 4 months in SAMP8 and became progressively more pronounced with age. Because a reduction in anxiety was also found in SAMR1 at a much older age (20 months), it was concluded that behavioral abnormalities of SAMP8 was an earlier manifestation of age-related emotional disorders. By comparing SAMP8 and SAMR1 at 4 months and 15 months, Markowska et al. (1998) also noted reduced anxiety by plus maze test, hyperactivity by open-field test, and an age-related impairment of sensorimotor performance.

Our study on the behavior of the two strains at five time points between 1 month and 10 months clearly demonstrated that hyperactivity and reduced anxiety were not aging-dependent behavioral abnormalities but were characteristic of young SAMP8 before the onset of cognitive decline. Reduced TH signaling resulting from downregulation of *dio2* overlaps in timing with behavioral alterations, suggesting a possible link between the two phenomena.

Two lines of evidence relate the developmental deficiency in TH signaling to attention deficit-hyperactivity disorder (ADHD) in humans. One is the high incidence of ADHD (40–70%) associated with generalized resistance to thyroid hormone (RTH), a rare genetic syndrome caused by mutations in the TH receptor β (TRβ) gene that result in reduced T3 binding (Hauser et al., 1993). RTH is characterized by elevated serum T4 and T3 concentrations, accompanied by normal or elevated level of thyroid-stimulating hormone (TSH) and by reduced responsiveness of the pituitary and peripheral tissues to TH. Knock-in mice expressing a human mutant TRβ allele (TRβPV) found in RTH exhibited hyperactivity, impaired learning, and altered responsiveness to methylphenidate resembling human ADHD (Siesser et al., 2005, 2006).

The second piece of evidence linking TH and ADHD comes from studies on preterm infants (Simic et al., 2009). Because the fetal thyroid does not produce significant amounts of TH until the third trimester in humans (Williams, 2008), most preterm infants experience a transient neonatal hypothyroidism during what should have been the later part of pregnancy in which maternal TH supply is still important. TH insufficiency is thus considered a major cause of neurocognitive deficits with reduced attention at 3 months of age (Simic et al., 2009). Attention-deficit and hyperactive behavior could also be reproduced in an animal model of perinatal hypothyroidism obtained by administering PTU to pregnant rats during pregnancy and lactation periods (Negishi et al., 2005). Although body weights at birth were comparable to those of euthyroid pups, offspring of PTU-treated dams showed a reduction in postnatal body weight increase. When tested behaviorally at the young adult stage (8 weeks of age), they exhibited hyperactivity, low anxiety, impaired learning, and shortened attention span compared with euthyroid animals.

Although SAMP8 mice have been considered as models of age-dependent cognitive disorders, our study shows that, at younger ages, they may serve as an interesting model of developmental disorders caused by local T3 deficiency. The present results also raise the possibility that accelerated senescence in SAMP8 mice may originate from subclinical deficits in TH signaling during development. Perturbations in the TH system can occur not only endogenously but also through environmental factors such as iodine or Se deficiency and intake of some chemicals (Takahashi et al., 2009), so studies on SAMP8 both at younger and at older ages should provide valuable insights into the role of the TH system in the development and maintenance of the CNS.

ACKNOWLEDGMENTS

We thank Mr. Eita Iwasaki and Mr. Shinpei Kikuma in the initial phase of the study.

REFERENCES

Arrojo e Drigo R, Bianco AC. 2011. Type 2 deiodinase at the crossroads of thyroid hormone action. Int J Biochem Cell Biol 43:1432–1441.

Bernal J. 2005. Thyroid hormones and brain development. Vitam Horm 71:95–122.

Bradford MM. 1976. A rapid and sensitive method for the quantitation of microgram quantities of protein utilizing the principle of protein-dye binding. Anal Biochem 72:248–254.

Butterfield DA, Poon HF. 2005. The senescence-accelerated prone mouse (SAMP8): a model of age-related cognitive decline with relevance to alterations of the gene expression and protein abnormalities in Alzheimer's disease. Exp Gerontol 40:774–783.

Butterfield DA, Howard BJ, Yatin S, Allen KL, Carney JM. 1997. Free radical oxidation of brain proteins in accelerated senescence and its modulation by N-tert-butyl-alpha-phenylnitrone. Proc Natl Acad Sci U S A 94:674–678.

Calzà L, Fernandez M, Giuliani A, D'Intino G, Pirondi S, Sivilia S, Paradisi M, Desordi N, Giardino L. 2005. Thyroid hormone and remyelination in adult central nervous system: a lesson from an inflammatory-demyelinating disease. Brain Res Rev 48:339–346.

Calzà L, Fernandez M, Giardino L. 2010. Cellular approaches to central nervous system remyelination stimulation: thyroid hormone to promote myelin repair via endogenous stem and precursor cells. J Mol Endocrinol 44:13–23.

Colas D, Cespuglio R, Sarda N. 2005. Sleep wake profile and EEG spectral power in young or old senescence accelerated mice. Neurobiol Aging 26:265–273.

Davis JD, Tremont G. 2007. Neuropsychiatric aspects of hypothyroidism and treatment reversibility. Minerva Endocrinol 32:49–65.

Del Valle J, Duran-Vilaregut J, Manich G, Casadesús G, Smith MA, Camins A, Pallàs M, Pelegrí C, Vilaplana J. 2010. Early amyloid

accumulation in the hippocampus of SAMP8 mice. J Alzheimers Dis 19:1303–1315.

Dentice M, Salvatore D. 2011. Deiodinases: the balance of thyroid hormone: local impact of thyroid hormone inactivation. J Endocrinol 209:273–282.

Farsetti A, Mitsuhashi T, Desvergne B, Robbins J, Nikodem VM. 1991. Molecular basis of thyroid hormone regulation of myelin basic protein gene expression in rodent brain. J Biol Chem 266:23226–23232.

Flood JF, Morley JE. 1992. Early onset of age-related impairment of aversive and appetitive learning in the SAM-P/8 mouse. J Gerontol 47:B52–B59.

Flood JF, Morley JE. 1993. Age-related changes in footshock avoidance acquisition and retention in senescence accelerated mouse (SAM). Neurobiol Aging 14:153–157.

Freitas BC, Gereben B, Castillo M, Kalló I, Zeöld A, Egri P, Liposits Z, Zavacki AM, Maciel RM, Jo S, Singru P, Sanchez E, Lechan RM, Bianco AC. 2010. Paracrine signaling by glial cell-derived triiodothyronine activates neuronal gene expression in the rodent brain and human cells. J Clin Invest 120:2206–2217.

Gereben B, Zavacki AM, Ribich S, Kim BW, Huang SA, Simonides WS, Zeöld A, Bianco AC. 2008. Cellular and molecular basis of deiodinase-regulated thyroid hormone signaling. Endocr Rev 29:898–938.

Hauser P, Zametkin AJ, Martinez P, Vitiello B, Matochik JA, Mixson AJ, Weintraub BD. 1993. Attention deficit-hyperactivity disorder in people with generalized resistance to thyroid hormone. N Engl J Med 328:997–1001.

Koibuchi N, Chin WW. 2000. Thyroid hormone action and brain development. Trends Endocrinol Metab 11:123–128.

Lamirand A, Pallud-Mothré S, Ramaugé M, Pierre M, Courtin F. 2008. Oxidative stress regulates type 3 deiodinase and type 2 deiodinase in cultured rat astrocytes. Endocrinology 149:3713–3721.

Markowska AL, Spangler EL, Ingram DK. 1998. Behavioral assessment of the senescence-accelerated mouse (SAM P8 and R1). Physiol Behav 64:15–26.

Martínez de Arrieta C, Morte B, Coloma A, Bernal J. 1999. The human RC3 gene homolog, NRGN contains a thyroid hormone-responsive element located in the first intron. Endocrinology 140:335–343.

Meier S, Bräuer AU, Heimrich B, Nitsch R, Savaskan NE. 2004. Myelination in the hippocampus during development and following lesion. Cell Mol Life Sci 61:1082–1094.

Miyamoto M, Kiyota Y, Yamazaki N, Nagaoka A, Matsuo T, Nagawa Y, Takeda T. 1986. Age-related changes in learning and memory in the senescence-accelerated mouse (SAM). Physiol Behav 38:399–406.

Miyamoto M, Kiyota Y, Nishiyama M, Nagaoka A. 1992. Senescence-accelerated mouse (SAM): age-related reduced anxiety-like behavior in the SAM-P/8 strain. Physiol Behav 51:979–985.

Murakami M, Tanaka K, Greer MA, Mori M. 1988. Anterior pituitary type II thyroxine 5′-deiodinase activity is not affected by lesions of the hypothalamic paraventricular nucleus which profoundly depress pituitary thyrotropin secretion. Endocrinology 123:1676–1681.

Negishi T, Kawasaki K, Sekiguchi S, Ishii Y, Kyuwa S, Kuroda Y, Yoshikawa Y. 2005. Attention-deficit and hyperactive neurobehavioural characteristics induced by perinatal hypothyroidism in rats. Behav Brain Res 159:323–331.

Nomura Y, Yamanaka Y, Kitamura Y, Arima T, Ohnuki T, Oomura Y, Sasaki K, Nagashima K, Ihara Y. 1996. Senescence-accelerated mouse. Neurochemical studies on aging. Ann N Y Acad Sci 786:410–418.

Oppenheimer JH, Schwartz HL. 1997. Molecular basis of thyroid hormone-dependent brain development. Endocr Rev 18:462–475.

Potter GB, Zarach JM, Sisk JM, Thompson CC. 2002. The thyroid hormone-regulated corepressor hairless associates with histone deacetylases in neonatal rat brain. Mol Endocrinol 16:2547–2560.

Siesser WB, Cheng SY, McDonald MP. 2005. Hyperactivity, impaired learning on a vigilance task, and a differential response to methylphenidate in the TRbetaPV knock-in mouse. Psychopharmacology 181:653–663.

Siesser WB, Zhao J, Miller LR, Cheng SY, McDonald MP. 2006. Transgenic mice expressing a human mutant beta1 thyroid receptor are hyperactive, impulsive, and inattentive. Genes Brain Behav 5:282–297.

Simic N, Asztalos EV, Rovet J. 2009. Impact of neonatal thyroid hormone insufficiency and medical morbidity on infant neurodevelopment and attention following preterm birth. Thyroid 19:395–401.

Simonides WS, Mulcahey MA, Redout EM, Muller A, Zuidwijk MJ, Visser TJ, Wassen FW, Crescenzi A, da-Silva WS, Harney J, Engel FB, Obregon MJ, Larsen PR, Bianco AC, Huang SA. 2008. Hypoxia-inducible factor induces local thyroid hormone inactivation during hypoxic-ischemic disease in rats. J Clin Invest 118:975–983.

Takahashi M, Negishi T, Tashiro T. 2008. Identification of genes mediating thyroid hormone action in the developing mouse cerebellum. J Neurochem 104:640–652.

Takahashi M, Negishi T, Imamura M, Sawano E, Kuroda Y, Yoshikawa Y, Tashiro T. 2009. Alterations in gene expression of glutamate receptors and exocytosis-related factors by a hydroxylated-polychlorinated biphenyl in the developing rat brain. Toxicology 257:17–24.

Takeda T. 2009. Senescence-accelerated mouse (SAM) with special references to neurodegeneration models, SAMP8 and SAMP10 mice. Neurochem Res 34:639–659.

Takeda T, Hosokawa M, Takeshita S, Irino M, Higuchi K, Matsushita T, Tomita Y, Yasuhira K, Hamamoto H, Shimizu K, Ishii M, Yamamuro T. 1981. A new murine model of accelerated senescence. Mech Aging Dev 17:183–194.

Tanaka J, Okuma Y, Tomobe K, Nomura Y. 2005. The age-related degeneration of oligodendrocytes in the hippocampus of the senescence-accelerated mouse (SAM) P8: a quantitative immunohistochemical study. Biol Pharm Bull 28:615–618.

Tha KK, Okuma Y, Miyazaki H, Murayama T, Uehara T, Hatakeyama R, Hayashi Y, Nomura Y. 2000. Changes in expressions of proinflammatory cytokines IL-1beta, TNF-alpha and IL-6 in the brain of senescence-accelerated mouse (SAM) P8. Brain Res 885:25–31.

Tomobe K, Nomura Y. 2009. Neurochemistry, neuropathology, and heredity in SAMP8: a mouse model of senescence. Neurochem Res 34:660–669.

Tomobe K, Shinozuka T, Kuroiwa M, Nomura Y. 2012. Age-related changes of Nrf2 and phosphorylated GSK-3β in a mouse model of accelerated aging (SAMP8). Arch Gerontol Geriatr 54:e1–e7.

Williams GR. 2008. Neurodevelopmental and neurophysiological actions of thyroid hormone. J Neuroendocrinol 20:784–794.

Yagi H, Katoh S, Akiguchi I, Takeda T. 1988. Age-related deterioration of ability of acquisition in memory and learning in senescence accelerated mouse: SAM-P/8 as an animal model of disturbances in recent memory. Brain Res 474:86–93.

新聞　（第3種郵便物認可）

「安心して鯨食べて」

国のセンター所長 毛髪濃度高いが中毒なし

太地・水銀と健康調査報告会

水銀の健康への影響について説明する国立水俣病総合研究センターの職員（太地町で）

太地町で30日夜、開かれた「水銀と健康影響に関する調査」の住民報告会では、2年前の調査結果同様、住民の水銀濃度は高いものの、水銀中毒を疑わせる症状はなかったことが報告された。調査した国立水俣病総合研究センターの阿部重一所長は「安心してクジラを食べて下さい」と説明。地元住民からは「安心した」との声が相次いだが、識者からは胎児への影響を懸念する意見もあり、町は今後、胎児期の摂取の影響が出やすいとされる小学1、2年生を対象とした調査を行うとしている。

町公民館で開かれた報告会には住民やクジラ漁関係者、町幹部ら約100人が出席。前回の調査で毛髪に含まれる水銀値が高かった人を中心にした194人に対する調査結果が示された。

阿部所長は、毛髪水銀濃度は国内平均の約7倍の数値となったものの、メチル水銀中毒を疑わせる症状は見られなかったと報告。「水銀濃度の値が高いのは確かだが、マグロやブリをよく食べる地域でも高い。クジラはメチル水銀が高いが、セレンも高く、両者がくっつくと無害化する可能性がある」と述べた。

週に1、2回はクジラを食べ、28㎝の毛髪水銀値が検出されたという町内の調理師女性(58)は「結果を聞いて安心した。健康に影響がないのなら、これからもクジラを食べたい」とほっとした様子。クジラ漁に従事している小畑充規さん(45)は「83歳で現役の仲間もいるがぴんぴんしている。健康被害がないことを証明してもらってありがたい」と喜んだ。

三軒一高町長は、「さらに調査を進め、7月にパナマで開かれる国際捕鯨委員会（IWC）総会で調査結果を世界に発信したい」と意気込んだ。

しかし、愛媛大沿岸環境科学研究センターの田辺信介教授（環境化学）は「水銀の影響を最も受けやすいのは胎児なので、今後、妊婦を中心にした調査や食事指導を行う必要があるのでは」と指摘。

化学物質が妊婦に与える影響を調べる国の研究に携わっている成田正明・三重大大学院医学系研究科教授は「有機水銀の胎児への影響はわかっていないことが多く、さらなる研究が必要」と話している。

識者 胎児への影響懸念

小学低学年 町が調査へ

読売新聞　2012年6月1日

子どもの発達障害

子どもがじっとしていられない。こだわりが強すぎる。これは個人差の範囲内なのか―。近年、ニュースや本で話題にのぼる発達障害。三重大付属病院（津市）と紀南病院（御浜町）で小児発達外来を担当する三重大院医学系研究科の成田正明教授（51）に、障害の特徴や治療の最前線について聞いた。（小柳悠志）

あの人に聞いてみよう

早期発見と支援必要

三重大院医学系研究科教授

成田正明さん（51）

―発達障害とは。

人との関わりが苦手な自閉症、落ち着きがない注意欠陥多動性障害（ADHD）、読み書き計算など特定の分野が苦手な学習障害（LD）などの総称で、近年増加しているとされます。「障害」と名がつくものの、外見からうかがい知れない症状のため、日々の生活で苦労が多いといえます。

―気を付けるべきことは。

発達障害は、何らかの原因による生まれながらの脳機能の障害です。生後の環境や育て方で生じるものではありません。早期発見と適切な支援が必要です。一方、子どもであればおかしくない程度のこだわりが見られただけで、保護者や保育士、医師までもが「この子は発達障害では？」と思い込むことも多くあります。受診で何科に行けばよいか迷う人も少なくありません。児童精神科医と小児科医で対応が異なることもあります。

―成田教授の紀南病院での取り組みは。

看護師や言語聴覚士らと、患者さんの短所長所の把握や社会への適応訓練を行っています。障害に対する周囲の理解があれば、訓練の効果は上がります。

―今後の研究の方向性について。

生まれながらの原因とされる発達障害ですが、妊娠中のどのようなことが原因で引き起こされるかわかっていません。遺伝的な因子の関与も指摘されています。根本的な治療法はないといわれますが、本当にそうなのか、予防法はないのかなども研究しています。

なりた・まさあき　1961年神戸市生まれ。87年に広島大医学部を卒業し、2006年三重大医学部教授。医学博士。日本小児科学会認定小児科専門医。日本小児神経学会認定小児神経専門医。専門は発生学、小児神経学。09年から厚生労働省の研究班班長として、三重大を拠点に発達障害研究に取り組む。

中日新聞三重版　2013年1月6日

NHKテレビ“視点論点”
「化学物質ホルムアルデヒドと健康」
三重大学　成田正明
2012年6月15日放送

・こんにちは、三重大学の成田正明です。

・利根川水系の浄水場で、水質基準を超える有害化学物質ホルムアルデヒドが相次いで検出され、取水制限・断水などの影響があり、原因解明に向け調査が進んでいます。
・この問題では、汚染の原因は、ホルムアルデヒドが直接、利根川水系に流れこんだのではなく、ヘキサメチレンテトラミンという、塩素と反応してホルムアルデヒドを生成する化学物質がどこからか利根川水系に流れこんだと考えられると、環境省・厚生労働省は発表しています。
・しかしながらヘキサメチレンテトラミンは無論、ホルムアルデヒドという、このいずれもいわゆる化学物質、一般には耳慣れない単語なのではないでしょうか。

・私は厚生労働省の化学物質リスク研究事業の班長として、環境中の化学物質の健康への影響について研究して参りました。
・そこで本日は、化学物質ホルムアルデヒドと健康について論じたいと思います。

・まず化学物質に関してですが、ひとことに化学物質と申しましても様々な意味で用いられている用語です。
・一般的には「化学物質を含まない安全な食品」などという言葉のとおり、食品添加物のような、人工的に合成された、有害な作用を持つ物質をイメージすることが多いといえますが、化学物質には人工的に作られたもののほか、鉄や鉛など重金属など、もともと自然界に存在するもの、さらには薬剤・アルコールも含まれます。
・これらの化学物質はわかっているだけでも3000万種類にも及び、その種類・工業生産量ともに増加しています。
・特に工業的につくられた化学物質、というと、有害・危険、というイメージがありますが、日常的に利便性や有益性をもたらすもの、たとえばプラスチックや薬なども化学物質と言え、私たちが健康で豊かな生活を送るのに欠かせないものも少なくありません。
・さてホルムアルデヒドですが、化け学的には、無色の、強い刺激臭のある気体です。ホルムアルデヒドの水溶液はホルマリンと呼ばれ、この呼び方なら、ホルマリン漬けの臓器など、一般にも耳にされたことは多いのではないでしょうか。
・ホルムアルデヒドの用途としては、今 申し上げたあげた臓器などの保存の他、接着剤・塗料など建築資材や家具にも安価なため広く用いられています。
・しかしホルムアルデヒドは建築資材から空気中に容易に放出されます。そのため低濃度でも新築の住居などで、頭痛・めまい・のどの痛みなどの症状が出るシックハウス症候群の原因物質のひとつとして知られています。

・ホルムアルデヒドの毒性としてまず第1に挙げておかなければならないのが、急性毒性として目やのどなどの粘膜への急性毒性、即ち、呼吸器系や目、のどなどへ激しい刺激を与え、炎症を引き起こすことです。

・さらに恐ろしいことに、ホルムアルデヒドには発癌性があることも指摘されています。

・このようにホルムアルデヒドには生活のための有用性の反面、人体へはさまざまな毒性があるため、種々の法的規制があります。

・まず毒物及び劇物取締法により医薬用外劇物に指定されています。ホルムアルデヒドは従来からも特定化学物質の第３類物質、即ち大量漏洩により急性障害を引きおこす物質に指定されていましたが、平成19年の労働安全衛生法、及び特定化学物質障害予防規則の改正で、微量の曝露でがん等の慢性障害を引きおこす第２類物質に引き上げられました。その濃度の作業環境測定も義務付けられています。

・また水質汚濁防止法というホルムアルデヒドなどの有害物質の排出を規制する法律もありますが、その一方、ヘキサメチレンテトラミンのような化学反応でホルムアルデヒドが産出される物質までは水質汚濁防止法では規制されていないのが現状のようです。

・これらの法律は通常、工業産業に従事する労働者を対象として想定されたものですが、実はホルムアルデヒドを取り扱う労働者はそれだけではありません。

・私は大学医学部の教員であり、医学部では研究のほか、教育では医学部生の解剖学教育にも従事しています。ご存じのように大学の医学部には解剖実習があり、解剖体の防腐処置として通常ホルムアルデヒドが用いられており、従ってこの場もまた規制の対象区域ということになります。

・その結果、解剖実習室内でも、他の作業場と同様、ホルムアルデヒド管理濃度を０．１ppm 以下とすることが求められており、私の所属する三重大学では解剖実習室にはへや全体の強力な換気のほか、解剖体から発散されるホルムアルデヒドを学生が鼻に吸い込む前に水際でエアカーテンのような要領で除去するホルマリン除去装置をいち早く導入しています。

・このように、ホルムアルデヒドという化学物質は、現代社会でさまざまな用途・ニーズがあるものの、人体へは深刻な被害をもたらすため、厳しい法規制のもとで可能な限り低い濃度での使用が求められているといえます。

・ここで大切なことは、法規制では問題とならないような低い濃度のホルムアルデヒドでもまた人体に悪影響をもたらすのではないかといった漠然とした不安が蔓延することです。

・現代社会では、ホルムアルデヒドを一切用いないで生活することは困難だからです。

・それではどうしたらよいのでしょうか。

・それにはホルムアルデヒドが、どの程度の曝露なら人体へどのような影響がでるかを科学的に明らかにする以外にありません。

・私は、平成２１年より私を代表として、厚生労働省、化学物質リスク研究事業の研究班を組織し、化学物質の人体への影響、とくに成人では問題とならないような濃度であっても胎児期には影響があるかも知れないと考え、妊娠と化学物質について研究して参りました。研究では、疫学調査や、臨床データ、動物実験を通して、ホルムアルデヒドはじめ様々な化学物質の人体への影響のメカニズムを明らかにしていきたいと思います。
・シックハウス症候群についても客観的な診断技術を確立していきたいと考えています。
・特にホルムアルデヒドの胎児への影響は全くと言っていいほどわかっておらず、大人では安全だという量でも、子どもや妊婦、即ち胎児にとってはそうではないということは十分あり得るわけで、このあたりを私の研究班で明らかにしたいと思っています。
・次に重要なのは、これらから得た科学に基づいた正しい結果を広く国民に知ってもらうことです。
・「この化学物質は危険だ」などの単発的な結果の集まりでは、ただ化学物質が危険という認識のみが広がってしまいます。風評被害も心配です。私たちの身の回りにはどんな化学物質が存在し、どんな性質があるのかも知る必要があります。化学物質を使うにあたり、無駄な使い方をせず、有効に使うことは、人体への影響だけでなく、環境への影響をも軽減させることにもつながります。
・科学に基づいた証拠の積み重ねが必要です。
・科学に基づいた政策が具体化されることによって初めて、安全・安心な社会の実現に結びつきます。
・これこそが今、科学研究に求められているものではないでしょうか。